



One-pot multi-component synthesis of novel chromeno[4,3-b]pyrrol-3-yl derivatives as alpha-glucosidase inhibitors

Malihe Karami¹ · Alireza Hasaninejad¹ · Hossein Mahdavi² · Aida Iraj^{3,4} · Somayeh Mojtabavi⁵ · Mohammad Ali Faramarzi⁴ · Mohammad Mahdavi⁶

Received: 2 August 2021 / Accepted: 6 October 2021 / Published online: 25 October 2021
© The Author(s), under exclusive licence to Springer Nature Switzerland AG 2021

Abstract

A green and efficient one-pot multi-component protocol was developed for the synthesis of some novel dihydrochromeno[4,3-b]pyrrol-3-yl derivatives through the reaction of arylglyoxals, malono derivatives, and different 4-amino coumarins in ethanol at reflux condition. In this method, all products were obtained in good to excellent yield. Next, all synthesized derivatives were evaluated for their α -glucosidase inhibitory activity. Most of the compounds displayed potent inhibitory activities with IC_{50} values in the range of 48.65 ± 0.01 – 733.83 ± 0.10 μ M compared to the standard inhibitor acarbose ($IC_{50} = 750.90 \pm 0.14$ μ M). The kinetic study of compound **5e** as the most potent derivative ($IC_{50} = 48.65 \pm 0.01$ μ M) showed a competitive mechanism with a K_i value of 42.6 μ M. Moreover, docking studies revealed that dihydrochromeno[4,3-b]pyrrol-3-yl effectively interacted with important residues in the active site of α -glucosidase.

Keywords Chromeno[4,3-b]pyrrol · α -glucosidase inhibitor · Multi-component reactions · Molecular docking · Synthesis

Introduction

Multi-component reactions (MCRs) are convergent reactions in which three or more raw materials react together to form a product so that all or most of the atoms form the new product [1]. MCRs are of particular importance because of their advantages such as simplicity of operation, reduction of separation and treatment steps, minimization of energy,

time, cost, and waste generation [2–5]. Therefore, many researchers in the field of pharmaceutical, biological, and organic chemistry have considered the design and use of MCRs.

Type 2 diabetes mellitus (T2DM) is recognized as one of the most extensive global health challenges in the modern world affecting approximately 462 million individuals corresponding to 6.28% of the world's population with over 1 million deaths per year [6, 7]. Diabetes is also a risk factor for cardiovascular disease, cognitive decline, and Alzheimer's dementia [8]. The concerning trends in incidence, prevalence, and mortality of T2DM as well as its economical burden promote researchers to develop new agents to reduce exposure to high glucose levels in the postprandial state [9].

In this regard, α -glucosidase is an attractive target. α -glucosidase (EC.3.2.1.20) is an essential enzyme located at the brush border of the intestines which hydrolyses the 1,4- α -glycosidic linkages of oligosaccharides, trisaccharides, and disaccharides to monosaccharides [10]. As a result, the increased level of simple sugars can be absorbed into the blood from the intestine. With the help of the bloodstream, these simple sugars enter the cells and are converted into energy with the help of insulin. Without insulin (inadequate insulin secretion or insulin resistance), glucose stays in the bloodstream, keeping blood sugar levels high which

✉ Alireza Hasaninejad
a_hasaninejad@yahoo.com

¹ Department of Chemistry, Faculty of Sciences, Persian Gulf University, 7516913817 Bushehr, Iran

² School of Chemistry, College of Science, Uccniversity of Tehran, P.O.Box, 14155-6455 Tehran, Iran

³ Stem Cells Technology Research Center, Shiraz University of Medical Sciences, Shiraz, Iran

⁴ Central Research Laboratory, Shiraz University of Medical Sciences, Shiraz, Iran

⁵ Department of Pharmaceutical Biotechnology, Faculty of Pharmacy, Tehran University of Medical Sciences, P.O. Box 14155-6451, 1417614411 Tehran, Iran

⁶ Endocrinology and Metabolism Research Center, Endocrinology and Metabolism Research Institute, Tehran University of Medical Sciences, Tehran, Iran

leads to hyperglycemia, impaired glucose tolerance, and at late-stage type II diabetes [11–13].

α -glucosidase inhibitors are used to reduce the hydrolyze, digestion, and absorption of carbohydrates as well as suppress postprandial hyperglycemia [14]. In the last few years, various molecules have been reported as potential inhibitors of α -glucosidase with natural origin such as polyphenols, terpenoids, flavonoids, alkaloids, and saponins [15, 16]. Acarbose, as an FDA-approved α -glucosidase inhibitor, is administered orally to control blood sugar levels. Nojirimycin, miglitol, and voglibose are other market anti- α -glucosidase drugs for T2DM [17, 18]. Meanwhile, various synthetic small-molecules of α -glucosidase inhibitors have been developed bearing imidazole [19], pyrazoles [20], quinazolinone [21], isatin [22], xanthone [23], and azole [24] groups.

Coumarin-fused heterocycles are among the most interesting and widely used compounds because of their applications such as anti-tumour [25], antibacterial [26], antifungal [26], anticoagulant [27], anti-inflammatory [28], antiviral [28] and anti-HIV activities [29]. Among them, pyrrole-fused derivatives of coumarin are important classes of natural marine materials, and a number of them showed significant biological and medicinal properties (Fig. 1). Marine alkaloids Ningalin B and Lamellarin D with chromenopyrrole moiety in their structures demonstrate potential treatments in central nervous system disorders [30–34]. Also, Lamellarins D, K, and M are cytotoxic agents to a wide range of cancer cell lines. Recently, due to the biological importance of chromenopyrroles, the synthesis of this

type of compounds has been considered in different research groups [34–39].

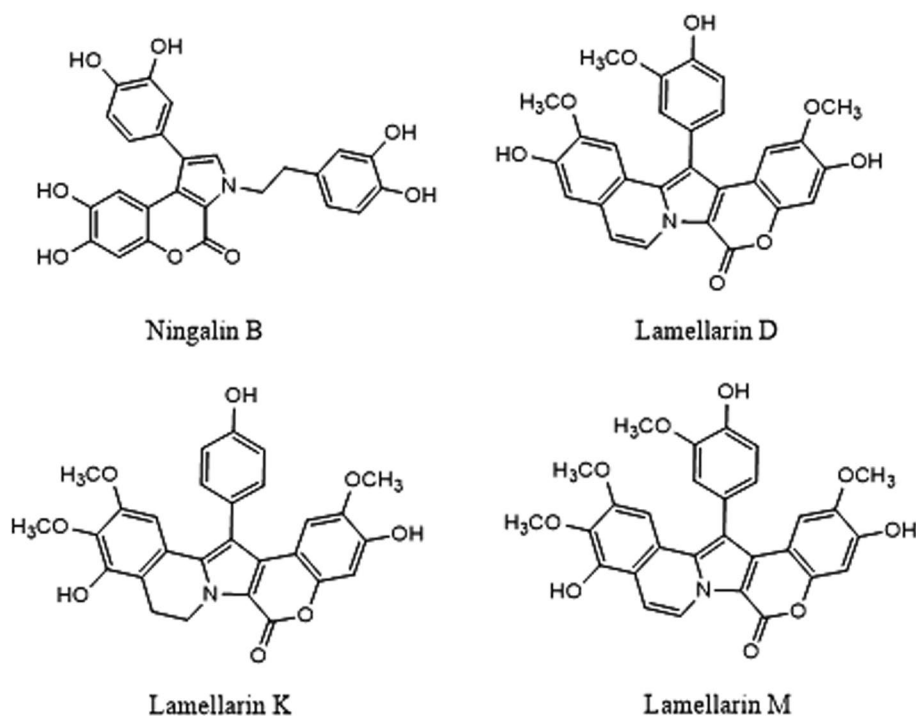
In continuation of our research on the synthesis of chromene and pyrrole [40–43], herein, a series of chromeno[4,3-b]pyrrol-3-yl were designed and synthesized through the MCRs. All derivatives were evaluated *in vitro* as possible anti- α -glucosidase agents, and the mode of inhibition was rationalized *in silico* through molecular docking studies.

Results and discussion

Design

To design a novel and efficient series of α -glucosidase inhibitors, the structural feature of some potent inhibitors with the possibility of MCRs synthesis reported in the literature was evaluated. Compounds containing chromenone (coumarin) rings have become an emerging anti-diabetic scaffold, recently (Fig. 2). Compound A was an attractive derivative bearing coumarin moiety with an IC_{50} value of 2.7 μ M. Interestingly, the replacement of the coumarin ring with other groups such as chloro, bromo, or nitro-phenyl showed a reduction in the inhibitory potency significantly [44]. In another study, coumarin containing thiazole-carbohydrates series demonstrated moderate to high potency with an IC_{50} value in the range of 6.2–81 μ M. Structure–activity relationship (SAR) studies proposed that electron-withdrawing substituents at phenyl of carbohydrazone

Fig. 1 Biologically active coumarin-fused pyrrole derivatives



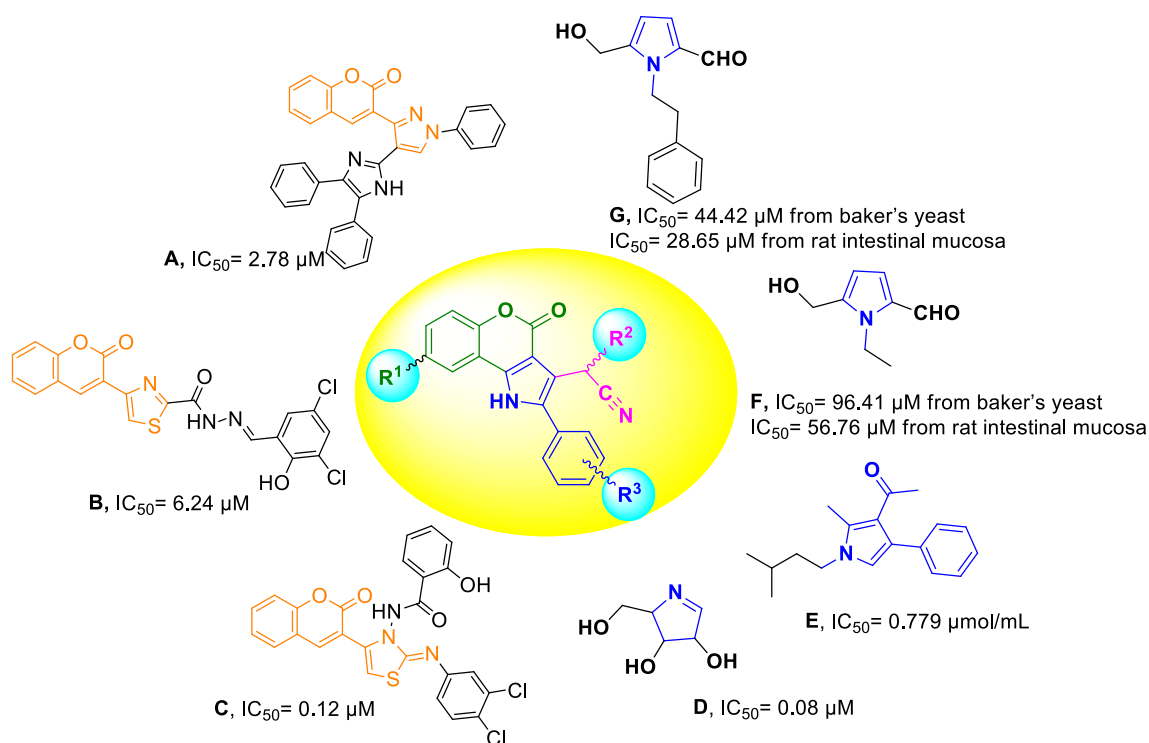


Fig. 2 Chemical structures of some reported α -glucosidase inhibitors and newly designed compound

improve inhibitory activity significantly. Docking analysis of compound **B** represented compact conformation through hydrophobic interactions of Pro240, Phe157, and Phe177 residues with coumarin ring [45]. Another series of coumarin-thiazoles were synthesized with an IC_{50} value in the range of 0.12–16.20 μM as compared to standard acarbose ($IC_{50} = 38.25 \mu M$). Docking study of the most potent derivative (compound **C**) displayed interactions with Asn241, Arg312, and Phe300. Also, polar interactions were observed in coumarin's oxygen and Asn241 residue [46].

On the other hands, pyrroles and their derivatives have attracted attention because of the ability of these compounds to act as glycosidase inhibitors so that pyrrole can mimic oxocarbocation intermediate structure, enable tight binding and strongly inhibit the enzyme [47]. Accordingly, there are some reports concerning α -glucosidase inhibitors possessing pyrrole rings. Compound **D** was reported to exhibit an IC_{50} of 0.08 μM against α -glucosidase [47]. Jadhaval et al. designed phenyl-1H-pyrrole derivatives and evaluated their α -glucosidase inhibitory activity. Compounds **E** showed excellent activity as compared to standard acarbose ($IC_{50} = 0.3 \mu mol/mL$). According to molecular docking study, the pyrrole ring of the molecule **E** occupied the cavity made by the residues, namely Trp58, Trp59, Glu63, Val163, and Leu165, while the phenyl ring occupied the pocket formed by the residues His101, Leu162, Arg195, Ala198, and Glu233 [48]. In another study, natural pyrrole-bearing

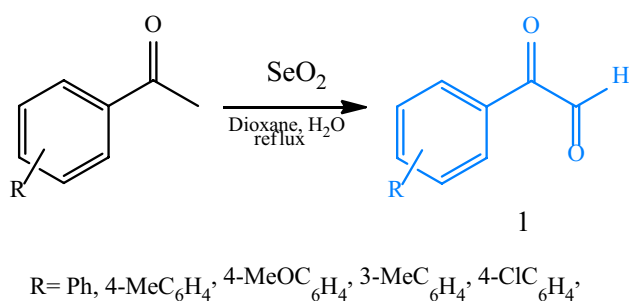
compounds were found in *G. frondosa* for the first time. Compounds **F** and **G** showed potent inhibition against α -glucosidase compared with acarbose with an IC_{50} value of 642.99 μM [49].

According to our limited literature review, compounds bearing both chromenone and pyrrole in particular, as anti- α -glucosidase agents have not been proposed yet. As a result, in the current study, molecular hybridization approaches were applied to design these targeted compounds which are anticipated to possess potent α -glucosidase inhibitory activity. Subsequently, fourteen chromeno[4,3-b]pyrrol derivatives were synthesized through MCRs and were evaluated against α -glucosidase. Moreover, the kinetic and docking studies of the most potent compound were performed to better understand the mode of inhibition and interactions with the enzyme.

Synthesis

Arylglyoxal derivatives were prepared from the oxidation of aryl methyl ketones using selenium dioxide as oxidant (Scheme 1) [50].

Then, to obtain the best reaction conditions for the synthesis of chromeno-pyrrole derivatives, the reaction between phenylglyoxal **1a** (1 mmol), malononitrile **2a** (1 mmol), and 4-aminocoumarin **3a** (1 mmol) was studied as a model reaction in different solvents and reaction temperatures. As can



Scheme 1 Preparation of arylglyoxals from the oxidation of aryl methyl ketones using SeO₂ as oxidant

Table 1 Effect of solvent and temperature on the reaction of phenylglyoxal, malononitrile and 4-aminocoumarin

Entry	Yield ^a (%)	Time (h)	Temp. (°C)	Solvent
1	Trace	8	Reflux	DMF
2	- ^b	8	rt	H ₂ O
3	Trace	8	Reflux	H ₂ O
4	50	8	Reflux	MeCN
5	60	8	70	Toluene
6	50	8	rt	EtOH
7	90	2	reflux	EtOH

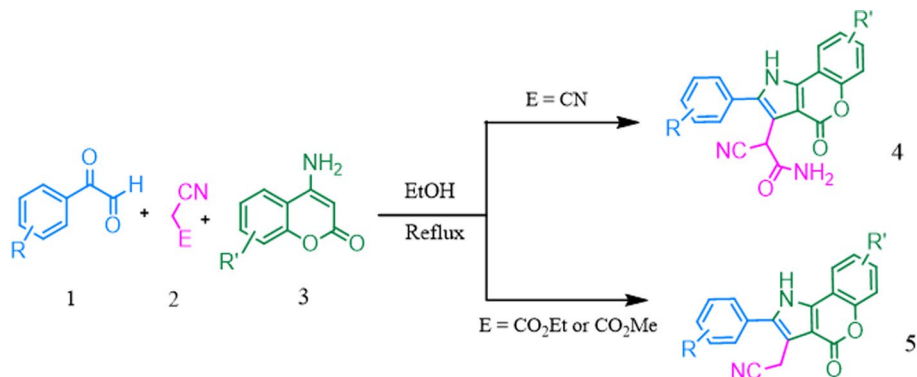
^aIsolated yields

^bIncomplete reaction with a number of unknown spots on TLC

be seen in Table 1, the best yield and shorter reaction times were obtained when the reaction was carried out in ethanol at reflux conditions (Table 1, entry 7).

Subsequently, the efficiency of this method was explored under the optimized reaction conditions for the condensation of different arylglyoxals, 4-amino coumarins, and alkyl malonates to furnish the related products (Scheme 2). The structural diversity of reactants is summarized in Fig. 3, and the results are displayed in scheme 2 and Table 2. It is noteworthy that product (4) was produced when malononitrile was used, on the other hands, when ethyl cyanoacetate or

Scheme 2 The synthesis of dihydrochromeno[4,3-*b*]pyrrol-3-yl derivatives via the reaction between arylglyoxal (1), malono derivatives (2) and 4-amino coumarin derivatives (3) in ethanol under reflux conditions



methyl cyanoacetate was used, product (5) was produced. As Table 2 indicates, a variety of arylglyoxals, alkyl malonates, and 4-aminocoumarins were successfully applied in this process to afford the corresponding chromeno[4,3-*b*]pyrrol-3-yl derivatives. These reactions were completed within 1–3 h with good to excellent yields (87–97%). As shown in Table 2, substitutions of the methyl or methoxy moiety on arylglyoxal aromatic ring improved the reactivity compared to chlorine counterparts.

A mixture of 4-aminocoumarin derivative (1 mmol), arylglyoxal (1 mmol) and malono derivative (1 mmol) was stirred in EtOH (5 mL) at reflux to obtain the desired product 4 or 5.

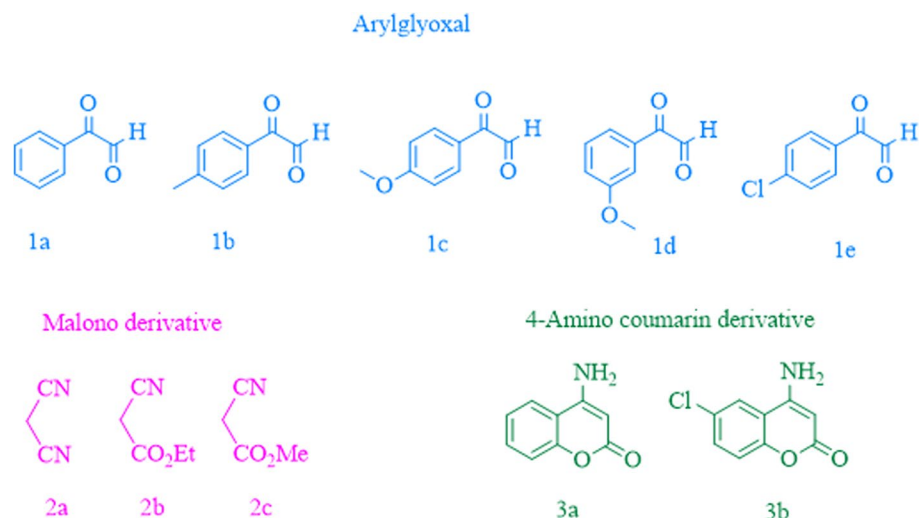
^b Isolated yields.

Based on the results, a plausible mechanism was proposed in (Scheme 3). Initially, under the Knoevenagel condensation reaction, arylglyoxal, and malono derivatives produced the intermediate 6. This intermediate then reacted with 4-amino coumarins to form intermediate 7. This intermediate was converted into 8 through the imine-enamine tautomerization, followed by N cyclization via attack to the C=O of arylglyoxal to produce 9. Then, hydrolysis of intermediate 9 gives product 4 when malononitrile was used as a starting material, and product 5 was formed when ethyl or methyl cyanoacetate were used as starting materials through decarboxylation of intermediate 10.

In vitro α -glucosidase inhibitory activity

Various dihydrochromeno[4,3-*b*]pyrrol-3-yl derivatives (4a–5f) were synthesized and evaluated against α -glucosidase. The results are summarized in Table 3. The majority of the tested compounds displayed potent α -glucosidase inhibitory activity, with IC₅₀ values in the range of 48.65 ± 0.01 to 733.83 ± 0.10 μ M, when compared to acarbose (IC₅₀ = 750.90 ± 0.14 μ M) as the positive control. Amongst, compound 5e represented the most potent α -glucosidase inhibition with IC₅₀ values of 48.65 ± 0.01 μ M. To better understand the SAR, synthesized compounds were divided

Fig. 3 Diversity elements employed for the synthesis of dihydrochromeno[4,3-b] pyrrole derivatives



into two main categories, **4a–e** (bearing CO-NH₂ at R¹) and **5a–f** (containing H at the R¹ position).

Evaluating the effect of R³ moiety on phenylpyrrole derivatives of **4a–e** showed that unsubstituted derivative (**4a**) had an anti- α -glucosidase activity with around fivefold improvement in the inhibitory potency compared to the positive control. The presence of chlorine atom at 4-position of phenyl ring (**4b**) improved the potency compared to the unsubstituted one. Replacement of chlorine with methyl (**4c**) as a moderate electron-donating group resulted in a significant reduction in the inhibitory activity. It is interesting to point out that the presence of a strong electron-donating group such as *meta*-MeO (**4d**) on the aryl ring improved inhibition compared to **4c**. The activity of **4e** (R² = Cl, R³ = 3-MeO) was slightly better than **4d** (R² = H, R³ = 3-MeO) indicated that the presence of chlorine group at R² can improve the inhibitory activity.

Evaluation in the second category (compounds **5a–f**) showed that unsubstituted phenyl ring with IC₅₀ value of 282.97 μ M (**5a**, R¹ = H, R² = H, R³ = H) had less activity in comparison with **4a** (R¹ = CO-NH₂, R² = H, R³ = H) counterpart. Disappointingly replacement of H at R² in **5a** with Cl (**5b**) moiety diminished the inhibitory activity completely. Unlike the previous group, the introduction of the methyl group at the 4-position of the phenyl ring (**5c**) improved inhibitory activity (IC₅₀ = 131.03 \pm 0.03 μ M). The replacement of methyl (**5c**) with chlorine (**5d**) as halogen electron-withdrawing group significantly improved the α -glucosidase inhibition with around fivefold increased in potency compared to **5a**. Compound **5e** having 4-methoxy group showed the most potent inhibitory activity (IC₅₀ = 48.65 μ M) among all synthesized compounds. Unexpectedly changing the position of MeO from *para* to *meta* caused a significant decline in potency. This result indicated the position, as well as the type of substitution on the phenyl ring, was responsible for outstanding α -glucosidase inhibition.

Overall, it can be understood that the presence of *para*-chlorine or *para*-methoxy at R³ position on phenylpyrrole pendant had the most dominant role to improve activity against α -glucosidase.

Enzyme kinetic studies

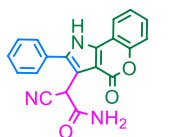
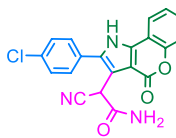
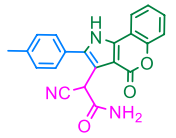
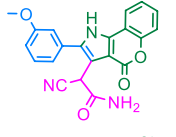
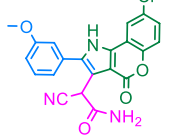
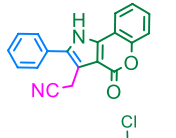
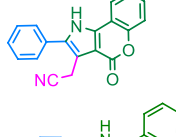
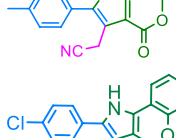
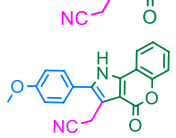
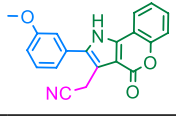
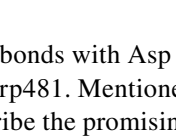
According to Fig. 4a, the Lineweaver–Burk plot showed that the K_m gradually increased and V_{max} remained unchanged with increasing inhibitor concentration indicating a competitive inhibition. The results showed that **5e** bond to the active site of the enzyme and competed with the substrate to bind to the active site. Furthermore, the plot of the K_m versus different concentrations of **5e** gave an estimate of the inhibition constant, K_i of 42.6 μ M (Fig. 4b).

Docking study

A molecular docking study was carried out to understand the possible interaction of **5e** with the residues of the α -glucosidase active site. To validate the docking procedure, the reference drug, acarbose, was first docked into the binding site of α -glucosidase using AutoDock Tools version 1.5.6. The docking protocol was successful to regenerate the native co-crystallized orientation of the docked ligand with an RMSD value of 1.41 Å.

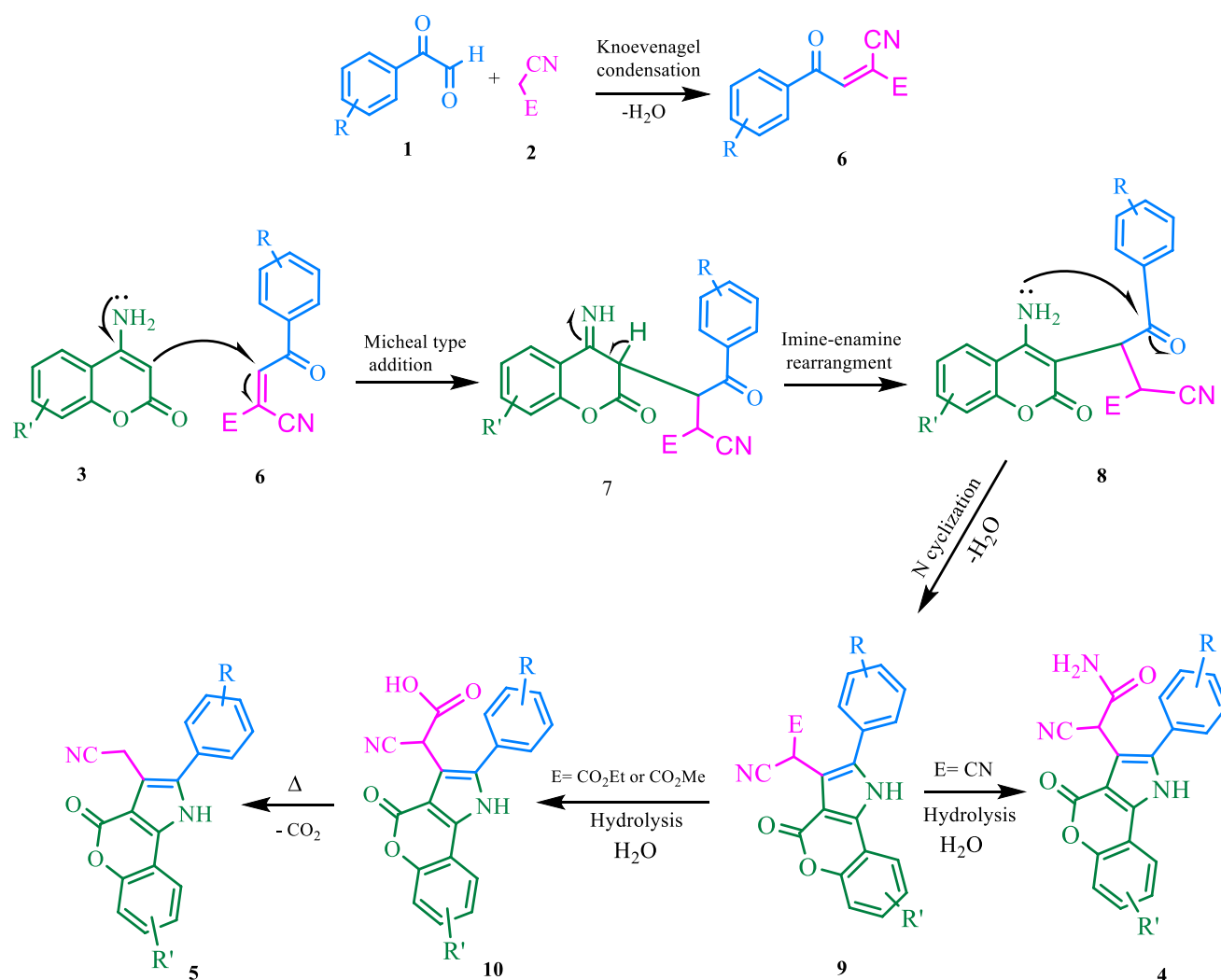
As can be seen in Fig. 5a, compound **5e** fitted well in the active site of the enzyme. The interaction of the best-docked conformation of **5e** with the residues of the active site is presented in Fig. 5b. Compound **5e** constructed three hydrogen bonds with the active site. The nitrogen of the acetonitrile moiety formed a hydrogen bond with Tyr292 residue and the oxygen of chromenone ring also recorded two hydrogen bonds with Leu283 and Ala284 residues of the 5NN8 which confirmed the efficacy of **5e** to induce the desired bioactivity. Also, chromenone ring

Table 2 One-pot, multi-component synthesis of dihydrochromeno[4,3-*b*]pyrrol derivatives in ethanol at reflux conditions.^[a]

Entry	Arylglyoxal	Malono derivatives	4-Amino coumarin	Product	Time (h)	Yield ^[b] (%)
4a	1a	2a	3a		2	90%
4b	1e	2a	3a		3	90%
4c	1b	2a	3a		1.5	92%
4d	1d	2a	3a		2	95%
4e	1d	2a	3b		2.5	93%
5a	1a	2b or 2c	3a		1.5	93%
5b	1a	2b or 2c	3b		2	92%
5c	1b	2b or 2c	3a		1	98%
5d	1e	2b or 2c	3a		2.5	90%
5e	1c	2b or 2c	3a		2	95%
5f	1d	2b or 2c	3a		2	97%

formed pi–sigma and pi–alkyl interactions with Ala555. Pi-anion interaction between the pyrrole ring and Asp282 fixed compound **5e** in the active site. At the other side of the molecule, methoxyphenyl moiety participated in two pi–anion interactions with Met519 and Asp616, two

carbon–hydrogen bonds with Asp 616 plus pi–pi-t-shaped interaction with Trp481. Mentioned interactions might be beneficial to describe the promising efficacy of compound **5e** against α -glucosidase.



Scheme 3 Proposed mechanism for the formation of products **4** and **5**

Conclusions

In the present study, novel series of chromeno[4,3-*b*]pyrrol-3-yl derivatives were synthesized through ordinal Knoevenagel/Michael/intramolecular cyclization sequences in ethanol without using any catalyst. The present procedure has the advantage that not only the reaction is performed under neutral conditions but also the reactants can be mixed without any prior activation or modification. High atom economy, simple procedure in the excellent yields, easy workup procedure, and mild reaction conditions are the main advantages of this method.

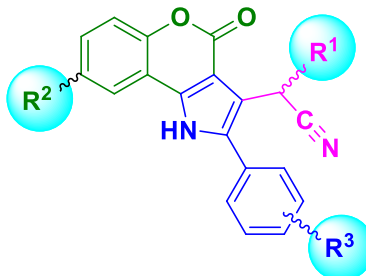
All synthesized compounds were then evaluated as α -glucosidase inhibitors. Among them, compound **5e** demonstrated the best inhibitory potency with an IC_{50} value of 48.65 μM which was 19 times more potent than acarbose as a standard inhibitor. Moreover, limited SARs of chromeno[4,3-*b*]pyrrol-3-yl derivatives showed that the

presence of *para*-methoxy or *para*-chlorine substituent on phenyl ring improved the inhibitory activity. Enzyme kinetic studies showed that compound **5e** is a competitive inhibitor with a K_i of 42.6 μM . Furthermore, the docking study was demonstrated that compound **5e** binds to the active site of the α -glucosidase through both hydrophobic and hydrogen bond interactions. The current study provides a new class of compounds for the development of novel α -glucosidase inhibitors.

Experimental section

Chemistry

All chemicals were purchased from Merck or Fluka chemical companies. The ^1H NMR (500 MHz) and ^{13}C NMR (125 MHz) were run on a Varian—Inova 500. Melting points

Table 3 α -glucosidase inhibitory activities of dihydrochromeno[4,3-b]pyrrol-3-yl derivatives^a


Compounds	R^1	R^2	R^3	IC_{50} (μM)
Acarbose				750.90 ± 0.14
4a	CO-NH ₂	H	H	151.94 ± 0.20
4b	CO-NH ₂	H	4-Cl	113.85 ± 0.01
4c	CO-NH ₂	H	4-Me	733.83 ± 0.10
4d	CO-NH ₂	H	3-MeO	223.06 ± 0.13
4e	CO-NH ₂	Cl	3-MeO	187.30 ± 0.17
5a	H	H	H	282.97 ± 0.27
5b	H	Cl	H	$750 <$
5c	H	H	4-Me	131.03 ± 0.03
5d	H	H	4-Cl	52.75 ± 0.77
5e	H	H	4-MeO	48.65 ± 0.01
5f	H	H	3-MeO	554.10 ± 0.06

^aData represented in terms of mean \pm SD

were recorded on a Stuart Scientific Apparatus SMP3 (UK) in open capillary tubes. Elemental analyses for C, H, and N were performed using a Thermo Finnigan FLASH EA. Reaction progress was screened by TLC using silicagel polygram SIL G/UV254 plates. Mass spectra were recorded on an Agilent Technology (HP) 5973 mass spectrometer operating at an ionization potential of 70 eV.

General procedure for the synthesis of arylglyoxal

18.5 g of selenium dioxide was dissolved in 100 mL of dioxane by warming to 50° C and stirring until all was in solution. To this solution was added 23 g of acetophenone derivatives and the reaction was refluxed for 4 h. The hot solution was decanted from the solid selenium, and the dioxane and water were removed by distillation through a short column at atmospheric pressure.

General procedure for the synthesis of chromeno[4,3-b]pyrrol-3-yl derivatives 4a-e, 5a-f

A mixture of arylglyoxal **1** (1 mmol), malono derivatives **2** (1 mmol), and 4-aminocoumarin derivatives **3** (1 mmol) was stirred in EtOH reflux (5 mL), and the solution was heated at reflux for the time given in Table 2. Upon completion as monitored by TLC, the reaction mixture was cooled, the

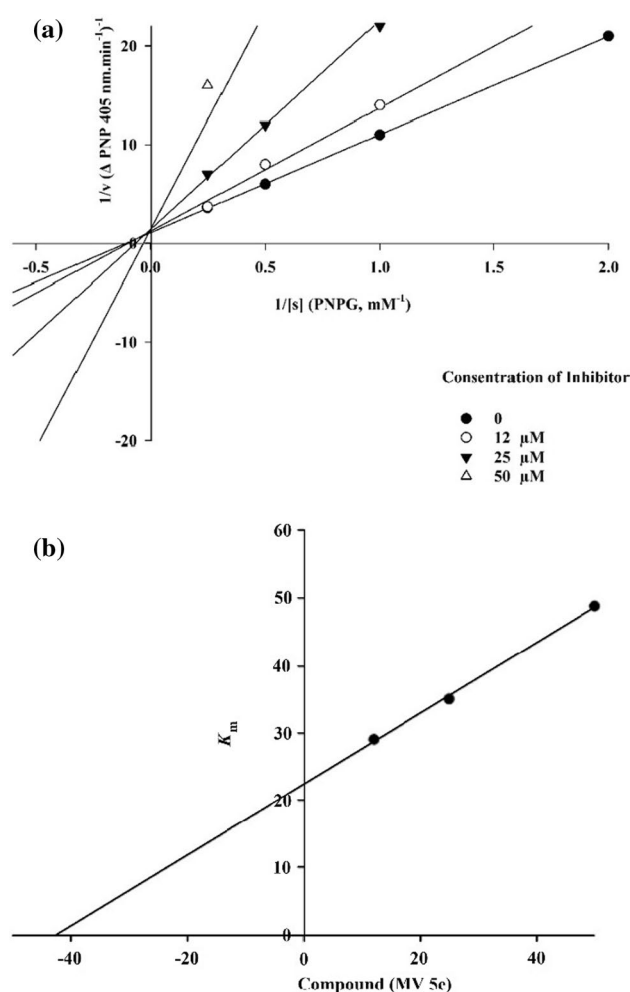


Fig. 4 Kinetics of α -glucosidase inhibition by **5e**. (a) The Lineweaver–Burk plot in the absence and presence of different concentrations of **5e**; (b) the secondary plot between K_m and various concentrations of **5e**

precipitate formed was filtered off and washed on the filter funnel with a small amount of ethanol to give pure products.

2-cyano-2-(4-oxo-2-phenyl-1,4-dihydrochromeno[4,3-b]pyrrol-3-yl)acetamide (4a):

White powder, m.p > 300 °C. ¹H NMR (DMSO-*d*₆, 500 MHz) δ (ppm): 5.47 (s, 1H), 7.38 (s, 1H), 7.43 (dd, $J = 1.5$ Hz, 7.5 Hz, 1H), 7.49–7.56 (m, 3H), 7.57–7.66 (m, 5H), 8.22 (dd, $J = 1.5$ Hz, 7.5 Hz, 1H), 12.97 (s, 1H). ¹³C NMR (DMSO-*d*₆, 125 MHz) δ (ppm): 35.55, 107.64, 109.29, 113.83, 117.42, 122.22, 124.91, 129.27, 129.33, 129.41, 129.56, 129.78, 130.24, 136.12, 136.81, 151.82, 158.50, 165.90. EI-MS (70 eV): m/z (%) = 340 (M^+ , 9), 325 (47), 300 (100). Anal. calcd for C₂₀H₁₃N₃O₃: C, 69.97; H, 3.82; N, 12.24%. Found: C, 69.97; H, 3.82; N, 12.24%.

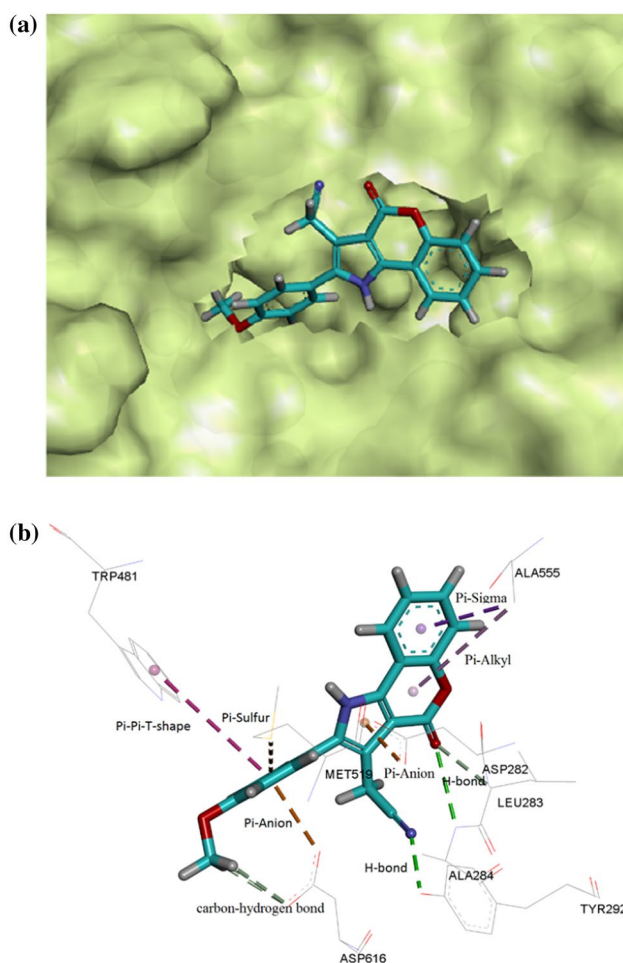


Fig. 5 The three-dimensional conformation of compound **5e** docked into the active site (A). Three-dimensional orientation of compound **5e** and important residues in the active site of 5NN8 (B). Hydrogen bonds are depicted in green dashed lines, Pi–Pi-T-shaped interactions are depicted in pink dashed lines, Pi–aryl interactions are depicted in dark pink dashed lines, Pi–anion interactions are depicted in orange dashed lines. Carbon–hydrogen bonds are depicted pale green dashed lines

2-(2-(4-chlorophenyl)-4-oxo-1,4-dihydrochromeno[4,3-b]pyrrol-3-yl)-2-cyanoacetamide (4b):

White powder, m.p > 300 °C, ^1H NMR (DMSO- d_6 , 500 MHz) δ (ppm): 6.43 (s, 1H), 7.41–7.45 (m, 1H), 7.49–7.67 (m, 5H), 7.71–7.74 (m, 2H), 8.16 (dd, $J=1.5$ Hz, 7.5 Hz, 1H), 13.31 (s, 1H). ^{13}C NMR (DMSO- d_6 , 125 MHz) δ (ppm): 20.03, 104.86, 106.92, 113.23, 117.53, 122.35, 125.05, 127.91, 129.71, 130.32, 131.12, 131.37, 134.89, 136.00, 136.90, 152.01, 157.77. EI-MS (70 eV): m/z (%) = 379 ($\text{M}^+ + 2$, 0.2), 377 (M^+ , 0.6), 359 (100). Anal. calcd for $\text{C}_{20}\text{H}_{12}\text{ClN}_3\text{O}_3$: C, 63.59; H, 3.20; N, 11.12%. Found: C, 63.58; H, 3.20; N, 11.10%.

2-cyano-2-(4-oxo-2-(p-tolyl)-1,4-dihydrochromeno[4,3-b]pyrrol-3-yl)acetamide (4c):

White powder, m.p > 300 °C, ^1H NMR (DMSO- d_6 , 500 MHz) δ (ppm): 2.41 (s, 3H), 5.46 (s, 1H), 7.37–7.43 (m, 4H), 7.47–7.59 (m, 5H), 8.21 (d, $J=7.5$ Hz, 1H), 12.90 (s, 1H). ^{13}C NMR (DMSO- d_6 , 125 MHz) δ (ppm): 21.39, 35.59, 107.63, 108.94, 113.37, 113.84, 117.37, 117.42, 122.18, 124.85, 127.40, 129.16, 129.66, 129.83, 130.25, 135.97, 136.89, 138.95, 151.77, 158.54, 165.97. EI-MS (70 eV): m/z (%) = 357 (M^+ , 1), 339 (7), 314 (100). Anal. calcd for $\text{C}_{21}\text{H}_{15}\text{N}_3\text{O}_3$: C, 70.58; H, 4.23; N, 11.76%. Found: C, 70.55; H, 4.20; N, 11.75%.

2-cyano-2-(2-(3-methoxyphenyl)-4-oxo-1,4-dihydrochromeno[4,3-b]pyrrol-3-yl)acetamide (4d):

White powder, m.p > 300 °C, ^1H NMR (DMSO- d_6 , 500 MHz) δ (ppm): 3.84 (s, 3H), 5.52 (s, 1H), 7.07 (d, $J=7.5$ Hz, 1H), 7.19–7.22 (m, 2H), 7.37–7.43 (m, 2H), 7.47–7.53 (m, 3H), 7.59 (s, 1H), 8.21 (d, $J=7.5$ Hz, 1H), 12.94 (s, 1H). ^{13}C NMR (DMSO- d_6 , 125 MHz) δ (ppm): 36.53, 56.63, 108.65, 110.34, 114.76, 115.70, 116.10, 118.39, 120.80, 122.36, 123.23, 125.89, 130.79, 131.44, 132.42, 137.04, 137.59, 152.77, 159.55, 160.72, 166.95. EI-MS (70 eV): m/z (%) = 373 (M^+ , 15), 356 (59), 330 (100). Anal. calcd for $\text{C}_{21}\text{H}_{15}\text{N}_3\text{O}_4$: C, 67.56; H, 4.05; N, 11.25%. Found: C, 67.51; H, 4.10; N, 11.25%.

2-(8-chloro-2-(3-methoxyphenyl)-4-oxo-1,4-dihydrochromeno[4,3-b]pyrrol-3-yl)-2-cyanoacetamide (4e):

White powder, m.p > 300 °C, ^1H NMR (DMSO- d_6 , 500 MHz) δ (ppm): 3.83 (s, 3H), 5.51 (s, 1H), 7.03–7.20 (m, 3H), 7.39–7.50 (m, 4H), 7.62 (s, 1H), 8.19 (d, $J=7.5$ Hz, 1H), 12.96 (s, 1H). ^{13}C NMR (DMSO- d_6 , 125 MHz) δ (ppm): 35.54, 55.66, 107.66, 109.37, 113.78, 114.74, 115.12, 117.35, 117.40, 121.39, 122.24, 124.89, 129.78, 130.43, 131.43, 136.04, 136.59, 151.79, 158.55, 159.73, 165.93. EI-MS (70 eV): m/z (%) = 409 ($\text{M}^+ + 2$, 0.2), 407 (M^+ , 0.6), 373 (15), 330 (100). Anal. calcd for $\text{C}_{21}\text{H}_{14}\text{ClN}_3\text{O}_4$: C, 61.85; H, 3.46; N, 10.30%. Found: C, 61.82; H, 3.43; N, 10.30%.

2-(4-oxo-2-phenyl-1,4-dihydrochromeno[4,3-b]pyrrol-3-yl)acetonitrile (5a):

White powder, m.p > 300 °C, ^1H NMR (DMSO- d_6 , 500 MHz) δ (ppm): 4.15 (s, 2H), 7.40–7.44 (m, 1H), 7.46–7.54 (m, 3H), 7.58–7.68 (m, 4H), 8.21 (dd, $J=1.5$ Hz, 7.5 Hz, 1H), 12.91 (s, 1H). ^{13}C NMR (DMSO- d_6 , 125 MHz) δ (ppm): 13.89, 107.69, 108.67, 113.78, 117.43, 118.93, 122.24, 124.84, 128.56, 129.10, 129.57, 129.70, 130.42,

135.41, 135.89, 151.82, 158.57. EI-MS (70 eV): m/z (%) = 300 (M^+ , 100), 271 (8), 255 (7). Anal. calcd for $C_{19}H_{12}N_2O_2$: C, 75.99; H, 4.03; N, 9.33%. Found: C, 76; H, 4.02; N, 9.30%.

2-(8-chloro-4-oxo-2-phenyl-1,4-dihydrochromeno[4,3-b]pyrrol-3-yl)acetonitrile (5b):

White powder, m.p > 300 °C, 1H NMR (DMSO- d_6 , 500 MHz) δ (ppm): 4.15 (s, 2H), 7.40–7.44 (m, 1H), 7.48–7.54 (m, 3H), 7.61–7.68 (m, 3H), 8.21 (dd, $J=1.5$ Hz, 7.5 Hz, 1H), 12.91 (s, 1H). ^{13}C NMR (DMSO- d_6 , 125 MHz) δ (ppm): 13.89, 107.68, 108.66, 113.76, 117.41, 118.93, 122.23, 124.82, 128.55, 129.09, 129.56, 129.68, 130.42, 135.40, 135.88, 151.81, 158.56. EI-MS (70 eV): m/z (%) = 336 ($M^+ + 2$, 0.2), 334 (M^+ , 0.7), 300 (M^+ , 100). Anal. calcd for $C_{19}H_{11}ClN_2O_2$: C, 68.17; H, 3.31; N, 8.37%. Found: C, 68.17; H, 3.31; N, 8.37%.

2-(4-oxo-2-(*p*-tolyl)-1,4-dihydrochromeno[4,3-b]pyrrol-3-yl)acetonitrile (5c):

White powder, m.p > 300 °C, 1H NMR (DMSO- d_6 , 500 MHz) δ (ppm): 2.42 (s, 3H), 4.13 (s, 2H), 7.40–7.45 (m, 3H), 7.46–7.53 (m, 2H), 7.55–7.57 (m, 2H), 8.21 (dd, $J=1.5$ Hz, 7.5 Hz, 1H), 12.84 (s, 1H). ^{13}C NMR (DMSO- d_6 , 125 MHz) δ (ppm): 13.89, 21.34, 107.65, 108.22, 113.78, 117.36, 118.96, 122.19, 124.76, 127.57, 128.37, 129.55, 130.09, 135.47, 135.69, 138.64, 151.76, 158.57. EI-MS (70 eV): m/z (%) = 314 (M^+ , 100). Anal. calcd for $C_{20}H_{14}N_2O_2$: C, 76.42; H, 4.49; N, 8.91%. Found: C, 76.40; H, 4.45; N, 8.90%.

2-(2-(4-chlorophenyl)-4-oxo-1,4-dihydrochromeno[4,3-b]pyrrol-3-yl)acetonitrile (5d):

Cream powder, m.p > 300 °C, 1H NMR (DMSO- d_6 , 500 MHz) δ (ppm): 4.17 (s, 2H), 7.40–7.43 (m, 1H), 7.45–7.54 (m, 2H), 7.65–7.74 (m, 4H), 8.185 (d, $J=7.5$ Hz, 1H), 12.93 (s, 1H). ^{13}C NMR (DMSO- d_6 , 125 MHz) δ (ppm): 13.78, 107.73, 109.21, 113.67, 117.44, 118.79, 122.26, 124.86, 129.27, 129.59, 129.59, 129.81, 130.25, 130.26, 133.78, 134.07, 136.06, 151.84, 158.50. EI-MS (70 eV): m/z (%) = 336 ($M^+ + 2$, 35), 334 (M^+ , 100). Anal. calcd for $C_{19}H_{11}ClN_2O_2$: C, 68.17; H, 3.31; N, 8.37%. Found: C, 68.14; H, 3.28; N, 8.4%.

2-(2-(4-methoxyphenyl)-4-oxo-1,4-dihydrochromeno[4,3-b]pyrrol-3-yl)acetonitrile (5e):

Cream powder, m.p > 300 °C, 1H NMR (DMSO- d_6 , 500 MHz) δ (ppm): 3.84 (s, 3H), 4.09 (s, 2H), 7.16 (d, $J=7.5$ Hz, 2H), 7.37–7.41 (m, 1H), 7.44–7.51 (m, 2H),

7.57–7.59 (m, 2H), 8.17 (d, $J=7.5$ Hz, 1H), 12.79 (s, 1H). ^{13}C NMR (DMSO- d_6 , 125 MHz) δ (ppm): 13.86, 55.80, 107.57, 107.73, 113.81, 115.01, 115.01, 117.37, 119.02, 122.13, 122.74, 124.77, 129.48, 129.95, 129.95, 135.46, 135.50, 151.73, 158.59, 159.97. EI-MS (70 eV): m/z (%) = 330 (M^+ , 100), 315 (26), 287 (28). Anal. calcd for $C_{20}H_{14}N_2O_3$: C, 72.72; H, 4.27; N, 8.48%. Found: C, 72.7; H, 4.25; N, 8.45%.

2-(2-(3-methoxyphenyl)-4-oxo-1,4-dihydrochromeno[4,3-b]pyrrol-3-yl)acetonitrile (5f):

White powder, m.p > 300 °C, 1H NMR (DMSO- d_6 , 500 MHz) δ (ppm): 3.86 (s, 3H), 4.14 (s, 2H), 7.06–7.09 (m, 1H), 7.19 (s, 1H), 7.22 (d, $J=7.5$ Hz, 1H), 7.39–7.54 (m, 4H), 8.20 (d, $J=7.5$ Hz, 1H), 12.87 (s, 1H). ^{13}C NMR (DMSO- d_6 , 125 MHz) δ (ppm): 13.93, 55.75, 107.68, 108.79, 113.74, 114.10, 114.63, 117.41, 118.97, 120.73, 122.27, 124.81, 129.70, 130.76, 131.64, 135.24, 135.83, 151.82, 158.56, 160.04. EI-MS (70 eV): m/z (%) = 330 (M^+ , 100), 287 (30). Anal. calcd for $C_{20}H_{14}N_2O_3$: C, 72.72; H, 4.27; N, 8.48%. Found: C, 72.7; H, 4.25; N, 8.45%.

α -glucosidase inhibition assay

α -glucosidase inhibition assay was performed exactly according to the previously reported procedure [20, 51–53].

Enzyme kinetic studies

The mode of inhibition of the most active compound (5e), identified with the lowest IC_{50} , was investigated against α -glucosidase at different concentrations of *p*-nitrophenyl α -D-glucopyranoside (2–10 mM) as substrate in the absence and presence of 5e at different concentrations (0, 12, 25, and 50 μ M). A Lineweaver–Burk plot was generated to identify the type of inhibition, and the Michaelis–Menten constant (K_m) value was determined from the plot between reciprocal of the substrate concentration ($1/[S]$) and reciprocal of enzyme rate ($1/V$) over various inhibitor concentrations. The experimental inhibitor constant (K_i) value was constructed by secondary plots of the inhibitor concentration $[I]$ versus K_m [52].

Molecular docking

The 3D structure of α -glucosidase with PDB ID: 5NN8 (EC: 3.2.1.20, resolution: 2.45 Å) was downloaded from the Brookhaven protein database (<https://www.rcsb.org/structure/5NN8>). Docking studies were performed using AutoDock Tools (version 1.5.6). The 3D structure of the selected compound was generated and energy minimized using hyperchem software and then converted to pdbqt

coordinate via Autodock Tools. Before docking, the water molecules and the inhibitor were removed from the protein. Then, using AutoDock Tools, polar hydrogen atoms were added, and Kollman charges were assigned. The active site is defined by the ligand of the protein crystal structure. The dimensions of the active site box were set at $60 \times 60 \times 60$ Å with flexible ligand dockings approach. The docked system was carried out by 50 runs of the AUTODOCK search by the Lamarckian genetic algorithm (LGA). The best position of **5e** was selected for analyzing the interactions against α -glucosidase. The results were visualized using Discovery Studio 2016 Client [22].

Supplementary Information The online version contains supplementary material available at <https://doi.org/10.1007/s11030-021-10337-w>.

Acknowledgements The authors thank Persian Gulf University Research Council for the financial support of this work.

Declarations

Conflicts of interest There are no conflicts to declare.

References

- Hasaninejad A, Zare A, Shekouhy M (2011) Highly efficient synthesis of triazolo [1, 2-a] indazole-triones and novel spiro triazolo [1, 2-a] indazole-tetraones under solvent-free conditions. *Tetrahedron* 67(2):390–400. <https://doi.org/10.1016/j.tet.2010.11.029>
- Zolfigol MA, Khazaei A, Zare A, Mokhlesi M, Hekmat-Zadeh T, Hasaninejad A, Derakhshan-Panah F, Moosavi-Zare AR, Keypour H, Dehghani-Firouzabadi AA (2012) Solid-supported sulfonic acid-containing catalysts efficiently promoted one-pot multi-component synthesis of β -acetamido carbonyl compounds. *J Chem Sci* 124(2):501–508. <https://doi.org/10.1007/s12039-011-0210-4>
- Zare A, Khanivar R, Hatami M, Mokhlesi M, Zolfigol MA, Moosavi-Zare AR, Hasaninejad A, Khazaei A, Khakyzadeh V (2012) Efficient Synthesis of 12-Aryl-8, 9, 10, 12-tetrahydrobenzo [α]-xanthen-11-ones using Ionic Liquid Pyrazinium Di (hydrogen sulfate)[Py (HSO₄)₂] as a Novel, Green and Homogeneous Catalyst. *J Mex Chem Soc* 56(4):389–397
- Edraki N, Firuzi O, Fatahi Y, Mahdavi M, Asadi M, Emami S, Divsalar K, Miri R, Iraj A, Khoshneviszadeh M, Firoozpour L, Shafiee A, Foroumadi A (2015) N-(2-(Piperazin-1-yl)phenyl) arylamide Derivatives as β -Secretase (BACE1) Inhibitors: Simple Synthesis by Ugi Four-Component Reaction and Biological Evaluation. *Arch Pharm* 348(5):330–337. <https://doi.org/10.1002/ardp.201400322>
- Hasaninejad A, Firoozi S, Mandegani F (2013) An efficient synthesis of novel spiro[benzo[c]pyrano[3,2-a]phenazines] via domino multi-component reactions using l-proline as a bifunctional organocatalyst. *Tetrahedron Lett* 54(22):2791–2794. <https://doi.org/10.1016/j.tetlet.2013.03.073>
- Wondafrash DZ, Desalegn TZ, Yimer EM, Tsige AG, Adamu BA, Zewdie KA (2020) Potential effect of hydroxychloroquine in diabetes mellitus: a systematic review on preclinical and clinical trial studies. *J Diabetes Res* 5(6):1–10. <https://doi.org/10.1155/2020/5214751>
- Khan MAB, Hashim MJ, King JK, Govender RD, Mustafa H, Al Kaabi J (2020) Epidemiology of Type 2 Diabetes - Global Burden of Disease and Forecasted Trends. *J Epidemiol Glob Health* 10(1):107–111. <https://doi.org/10.2991/jegh.k.191028.001>
- E. Blackburn, The Emerging Role of Pancreatic β -Cell Primary Cilia in Diabetes Mellitus, 4(28) (2021). https://opencommons.uconn.edu/srhonors_theses/777.
- Alssema M, Ruijgrok C, Blaak EE, Egli L, Dussort P, Vinoy S, Dekker JM, Denise Robertson M (2021) Effects of alpha-glucosidase-inhibiting drugs on acute postprandial glucose and insulin responses: a systematic review and meta-analysis. *Nutrition Diabetes*. <https://doi.org/10.1038/s41387-021-00152-5>
- Tundis R, Loizzo M, Menichini F (2010) Natural products as α -amylase and α -glucosidase inhibitors and their hypoglycaemic potential in the treatment of diabetes: an update. *Mini Rev Med Chem* 10(4):315–331. <https://doi.org/10.2174/138955710791331007>
- Khursheed R, Singh SK, Wadhwa S, Kapoor B, Gulati M, Kumar R, Ramanunni AK, Awasthi A, Dua K (2019) Treatment strategies against diabetes: Success so far and challenges ahead. *Eur J Pharmacol* 862:172625. <https://doi.org/10.1016/j.ejphar.2019.172625>
- Hakamata W, Kurihara M, Okuda H, Nishio T, Oku T (2009) Design and screening strategies for α -glucosidase inhibitors based on enzymological information. *Curr Top Med Chem* 9(1):3–12. <https://doi.org/10.2174/156802609787354306>
- Menteşe E, Baltaş N, Bekircan O (2019) Synthesis and kinetics studies of N'-(2-(3,5-disubstituted-4H-1,2,4-triazol-4-yl)acetyl)-6/7/8-substituted-2-oxo-2H-chromen-3-carbohydrazide derivatives as potent antidiabetic agents. *Arch Pharm* 352(12):1900227. <https://doi.org/10.1002/ardp.201900227>
- Bischoff H (1995) The mechanism of alpha-glucosidase inhibition in the management of diabetes. *Clin Invest Med* 18(4):303–311
- Ríos JL, Francini F, Schinella GR (2015) natural products for the treatment of type 2 diabetes mellitus. *Planta Med* 81(12–13):975–994. <https://doi.org/10.1055/s-0035-1546131>
- Wang L, Tan N, Wang H, Hu J, Diwu W, Wang X (2020) A systematic analysis of natural α -glucosidase inhibitors from flavonoids of *Radix scutellariae* using ultrafiltration UPLC-TripleTOF-MS/MS and network pharmacology. *BMC Complement Med Ther*. <https://doi.org/10.1186/s12906-020-2871-3>
- J. Djelmi, G. Desoye, *Diabetology of pregnancy*, Karger Medical and Scientific Publishers 2005.
- V. Mohan, R. Unnikrishnan, *World Clinics: Diabetology-Type 2 Diabetes Mellitus*, JP Medical Ltd 2014.
- Chaudhry F, Shahid W, Al-Rashida M, Ashraf M, Munawar MA, Khan MA (2021) Synthesis of imidazole-pyrazole conjugates bearing aryl spacer and exploring their enzyme inhibition potentials. *Bioorg Chem* 108:104686. <https://doi.org/10.1016/j.bioorg.2021.104686>
- Azimi F, Ghasemi JB, Azizian H, Najafi M, Faramarzi MA, Saghaei L, Sadeghi-Aliabadi H, Larijani B, Hassanzadeh F, Mahdavi M (2021) Design and synthesis of novel pyrazole-phenyl semicarbazone derivatives as potential α -glucosidase inhibitor: Kinetics and molecular dynamics simulation study. *Int J Biol Macromol* 166:1082–1095. <https://doi.org/10.1016/j.ijbiomac.2020.10.263>
- Sherafati M, Mirzazadeh R, Barzegari E, Mohammadi-Khanaposhtani M, Azizian H, Sadegh Asgari M, Hosseini S, Zabihi E, Mojtavani S, Ali Faramarzi M, Mahdavi M, Larijani B, Rastegar H, Hamedifar H, Hamed Hajimiri M (2021) Quinazolinone-dihydropyrano[3,2-b]pyran hybrids as new α -glucosidase inhibitors: Design, synthesis, enzymatic inhibition, docking study and prediction of pharmacokinetic. *Bioorganic Chemistry*. <https://doi.org/10.1016/j.bioorg.2021.104703>
- Shareghi-Boroujeni D, Iraj A, Mojtavani S, Faramarzi MA, Akbarzadeh T, Saeedi M (2021) Synthesis, in vitro evaluation, and molecular docking studies of novel hydrazineylideneindolinone

- linked to phenoxyethyl-1,2,3-triazole derivatives as potential α -glucosidase inhibitors. *Bioorg Chem* 111:104869. <https://doi.org/10.1016/j.bioorg.2021.104869>
23. Santos CMM, Freitas M, Fernandes E (2018) A comprehensive review on xanthone derivatives as α -glucosidase inhibitors. *Eur J Med Chem* 157:1460–1479. <https://doi.org/10.1016/j.ejmech.2018.07.073>
 24. Sari S, Barut B, Özel A, Saraç S (2020) Discovery of potent α -glucosidase inhibitors through structure-based virtual screening of an in-house azole collection. *Chem Biol Drug Des*. <https://doi.org/10.1111/cbdd.13805>
 25. Suzuki M, Nakagawa-Goto K, Nakamura S, Tokuda H, Morris-Natschke SL, Kozuka M, Nishino H, Lee K-H (2006) Cancer preventive agents Part 5 anti-tumor-promoting effects of coumarins and related compounds on Epstein-Barr virus activation and two-stage mouse skin carcinogenesis. *Pharmaceutical biology*. <https://doi.org/10.1080/13880200600686491>
 26. Kayser O, Kolodziej H (1999) Antibacterial activity of simple coumarins: structural requirements for biological activity. *Zeitschrift für Naturforschung C* 54(3–4):169–174. <https://doi.org/10.1515/znc-1999-3-405>
 27. Garazd YL, Kornienko E, Maloshtan L, Garazd M, Khilya V (2005) Modified coumarins. 17. Synthesis and anticoagulant activity of 3, 4-cycloannulated coumarin D-glycopyranosides. *Chem nat comp*. <https://doi.org/10.1007/s10600-005-0194-8>
 28. Kontogiorgis CA, Hadjipavlou-Litina DJ (2005) Synthesis and antiinflammatory activity of coumarin derivatives. *J Med Chem* 48(20):6400–6408. <https://doi.org/10.1021/jm0580149>
 29. Almerico AM, Diana P, Barraja P, Dattolo G, Mingoa F, Loi AG, Scintu F, Milia C, Puddu I, La Colla P (1998) Glycosidopyrroles Part I Acyclic derivatives: 1-(2-hydroxyethoxy) methylpyrroles as potential anti-viral agents. *Il Farmaco*. [https://doi.org/10.1016/s0014-827x\(97\)00002-5](https://doi.org/10.1016/s0014-827x(97)00002-5)
 30. Soenen DR, Hwang I, Hedrick MP, Boger DL (2003) Multidrug resistance reversal activity of key ningalin analogues. *Bioorg Med Chem Lett* 13(10):1777–1781. [https://doi.org/10.1016/s0960-894x\(03\)00294-4](https://doi.org/10.1016/s0960-894x(03)00294-4)
 31. Dubuffet T, Newman-Tancredi A, Cussac D, Audinot V, Loutz A, Millan MJ, Lavielle G (1999) Novel benzopyrano [3, 4-c] pyrrole derivatives as potent and selective dopamine D3 receptor antagonists. *Bioorg Med Chem Lett* 9(14):2059–2064. [https://doi.org/10.1016/s0960-894x\(99\)00312-1](https://doi.org/10.1016/s0960-894x(99)00312-1)
 32. Ridley CP, Reddy MVR, Rocha G, Bushman FD, Faulkner DJ (2002) Total synthesis and evaluation of lamellarin α 20-Sulfate analogues. *Bioorg Med Chem* 10(10):3285–3290. [https://doi.org/10.1016/S0968-0896\(02\)00237-7](https://doi.org/10.1016/S0968-0896(02)00237-7)
 33. Dubuffet T, Muller O, Simonet SS, Descombes J-J, Laubie M, Verbeuren TJ, Lavielle G (1996) Synthesis of new 3,4-disubstituted pyrrolidines as thromboxane A2/prostaglandin H2 (TP) receptor antagonists. *Bioorg Med Chem Lett* 6(4):349–352. [https://doi.org/10.1016/0960-894X\(96\)00021-2](https://doi.org/10.1016/0960-894X(96)00021-2). <https://doi.org/10.1016/j.rjcc.2018.03.001>
 34. Mukherjee S, Sarkar S, Pramanik A (2018) Synthesis of functionalized pyrrole fused coumarins under solvent-free conditions using magnetic nanocatalyst and a new route to polyaromatic indolocoumarins. *ChemistrySelect* 3:1537–1544. <https://doi.org/10.1002/slct.201703146>
 35. Yang X, Li Ch, Zhang F, Qi Ch (2021) An efficient domino strategy for synthesis of 3-substituted 4-oxo-4,5-dihydro-1H-pyrrolo[3,2-c]pyridine derivatives in water. *Mol Divers*. <https://doi.org/10.1007/s11030-021-10294-4>
 36. Mohammadi Ziarani Gh, Moradi R, Ahmadi T, Gholamzadeh P (2019). *Mol Divers*. <https://doi.org/10.1007/s11030-019-09918-7>
 37. Dai Ch, Xie Z, Qing X, Luo N, Wang C (2019) DBU-mediated annulation of 2-aryl-3-nitro-2H-chromenes with 1,3-cyclohexanediones for the synthesis of benzofuro[2,3-c]chromenone derivatives. *Mol Divers*. <https://doi.org/10.1007/s11030-019-09939-2>
 38. Yahyavi H, Heravi MM, Mahdavi M, Foroumadi A (2018) Iodine-catalyzed tandem oxidative coupling reaction: A one-pot strategy for the synthesis of new coumarin-fused pyrroles. *Tetrahedron Lett* 59(2):94–98. <https://doi.org/10.1016/j.tetlet.2017.11.055>
 39. Saha M, Pradhan K, Das AR (2016) Facile and eco-friendly synthesis of chromeno[4,3-b]pyrrol-4(1H)-one derivatives applying magnetically recoverable nano crystalline CuFe2O4 involving a domino three-component reaction in aqueous media. *RSC Adv* 6(60):55033–55038. <https://doi.org/10.1039/c6ra06979g>
 40. Hasaninejad A, Mojikhalifeh S, Beyrati M (2018) Highly efficient, catalyst-free, one-pot, pseudo five-component synthesis of novel pyrazoline-containing Schiff bases, metal complexes formation and computational studies via DFT method. *Appl Organomet Chem* 32(7):e4380. <https://doi.org/10.1002/aoc.4380>
 41. Mojikhalifeh S, Hasaninejad A (2018) Highly efficient, catalyst-free, one-pot, pseudo-seven-component synthesis of novel poly-substituted pyrazolyl-1,2-diazepine derivatives. *Organic Chemistry Frontiers* 5(9):1516–1521. <https://doi.org/10.1039/C8QO00210J>
 42. Beyrati M, Forutan M, Hasaninejad A, Rakovský E, Babaei S, Maryamabadi A, Mohebbi G (2017) One-pot, four-component synthesis of spiroindoloquinazoline derivatives as phospholipase inhibitors. *Tetrahedron* 73(34):5144–5152. <https://doi.org/10.1016/j.tet.2017.07.005>
 43. Maryamabadi A, Hasaninejad A, Nowrouzi N, Mohebbi G (2017) Green synthesis of novel spiro-indenoquinoline derivatives and their cholinesterases inhibition activity. *Bioorg Med Chem* 25(7):2057–2064. <https://doi.org/10.1016/j.bmc.2017.02.017>
 44. Chaudhry F, Naureen S, Huma R, Shaikat A, Al-Rashida M, Asif N, Ashraf M, Munawar MA, Khan MA (2017) In search of new α -glucosidase inhibitors: Imidazolopyrrole derivatives. *Bioorg Chem* 71:102–109. <https://doi.org/10.1016/j.bioorg.2017.01.017>
 45. Wang G, He D, Li X, Li J, Peng Z (2016) Design, synthesis and biological evaluation of novel coumarin thiazole derivatives as α -glucosidase inhibitors. *Bioorg Chem* 65:167–174. <https://doi.org/10.1016/j.bioorg.2016.03.001>
 46. Salar U, Taha M, Khan KM, Ismail NH, Imran S, Perveen S, Gul S, Wadood A (2016) Syntheses of new 3-thiazolyl coumarin derivatives, in vitro α -glucosidase inhibitory activity, and molecular modeling studies. *Eur J Med Chem* 122:196–204. <https://doi.org/10.1016/j.ejmech.2016.06.037>
 47. Witte JF, McClard RW (1991) Synthesis of a potent α -glucosidase inhibitor epimeric to fr 900483. *Tetrahedron Lett* 32(32):3927–3930. [https://doi.org/10.1016/0040-4039\(91\)2980591-S](https://doi.org/10.1016/0040-4039(91)2980591-S)
 48. Jadhav NC, Pahelkar AR, Desai NV, Telvekar VN (2017) Design, synthesis and molecular docking study of novel pyrrole-based α -amylase and α -glucosidase inhibitors. *Med Chem Res* 26(10):2675–2691. <https://doi.org/10.1007/s00040-017-1965-z>
 49. Chen S, Yong T, Xiao C, Su J, Zhang Y, Jiao C, Xie Y (2018) Pyrrole alkaloids and ergosterols from *Grifola frondosa* exert anti- α -glucosidase and anti-proliferative activities. *Journal of functional foods* 43:196–205. <https://doi.org/10.1016/j.jff.2018.02.007>
 50. Tiffany BD, Wright JB, Moffett RB, Heinzelman RV, Strube RE, Aspergren BD, Lincoln EH, White JL (1957) Antiviral compounds I Aliphatic glyoxals α -hydroxyaldehydes and related compounds. *J Am Chem Soc*. <https://doi.org/10.1021/JA01564A042>
 51. Mohammadi-Khanaposhthani M, Rezaei S, Khalifeh R, Imanparast S, Faramarzi MA, Bahadorikhalili S, Safavi M, Bandarian F, Esfahani EN, Mahdavi M (2018) Design, synthesis, docking study, α -glucosidase inhibition, and cytotoxic activities of acridine linked to thioacetamides as novel agents in treatment of type 2 diabetes. *Bioorg Chem* 80:288–295. <https://doi.org/10.1016/j.bioorg.2018.06.035>

52. Nikookar H, Mohammadi-Khanaposhtani M, Imanparast S, Faramarzi MA, Ranjbar PR, Mahdavi M, Larijani B (2018) Design, synthesis and in vitro α -glucosidase inhibition of novel dihydropyrano [3, 2-c] quinoline derivatives as potential anti-diabetic agents. *Bioorg Chem* 77:280–286. <https://doi.org/10.1016/j.bioorg.2018.01.025>
53. Azimi F, Azizian H, Najafi M, Hassanzadeh F, Sadeghi-Aliabadi H, Ghasemi JB, Faramarzi MA, Mojtavavi S, Larijani B, Saghaei L (2021) Design and synthesis of novel quinazolinone-pyrazole

derivatives as potential α -glucosidase inhibitors: Structure-activity relationship molecular modeling and kinetic study. *Bioorganic Chem.* <https://doi.org/10.1016/j.bioorg.2021.105127>

Publisher's Note Springer Nature remains neutral with regard to jurisdictional claims in published maps and institutional affiliations.